Published online 18 June 2007 *Nucleic Acids Research, 2007, Vol. 35, No. 13* ***4331–4346***
doi:10.1093/nar/gkm439

In vitro analysis of the interaction between the small RNA SR1 and its primary target *ahrC* mRNA

Nadja Heidrich[1], Isabella Moll[2] and Sabine Brantl[1,*]

[1]AG Bakteriengenetik, Friedrich-Schiller-Universität Jena, Philosophenweg 12, Jena D-07743, Germany and [2]Max F. Perutz Laboratories, Department of Microbiology and Immunobiology, University Departments at the Vienna Biocenter, Dr Bohrgasse 9/4, 1030 Vienna, Austria

Received April 20, 2007; Revised May 16, 2007; Accepted May 16, 2007

ABSTRACT

Small regulatory RNAs (sRNAs) from bacterial chromosomes became the focus of research over the past five years. However, relatively little is known in terms of structural requirements, kinetics of interaction with their targets and degradation in contrast to well-studied plasmid-encoded antisense RNAs. Here, we present a detailed *in vitro* analysis of SR1, a sRNA of *Bacillus subtilis* that is involved in regulation of arginine catabolism by basepairing with its target, *ahrC* mRNA. The secondary structures of SR1 species of different lengths and of the SR1/*ahrC* RNA complex were determined and functional segments required for complex formation narrowed down. The initial contact between SR1 and its target was shown to involve the 5′ part of the SR1 terminator stem and a region 100 bp downstream from the *ahrC* transcriptional start site. Toeprinting studies and secondary structure probing of the *ahrC*/SR1 complex indicated that SR1 inhibits translation initiation by inducing structural changes downstream from the *ahrC* RBS. Furthermore, it was demonstrated that Hfq, which binds both SR1 and *ahrC* RNA was not required to promote *ahrC*/SR1 complex formation but to enable the translation of *ahrC* mRNA. The intracellular concentrations of SR1 were calculated under different growth conditions.

INTRODUCTION

Small regulatory RNAs (sRNAs) are expressed in both prokaryotes and eukaryotes, primarily as posttranscriptional regulators. Over the past six years, about 70 sRNAs have been discovered in *E. coli*, and about 20 of them have been assigned a function. Many of these trans-encoded RNAs are involved in metabolic processes [e.g. Spot42, DsrA, RprA, RyhB, SgrS, GadY, reviewed in (1)] and at least eight sRNAs regulate the expression of membrane proteins [reviewed in (2)]. To date, relatively few systematic searches have been performed in Gram-positive bacteria. Among the recently discovered sRNAs in Gram-positive hosts are RatA from the *Bacillus subtilis* chromosome (3), which came up in a systematic search (4) together with 12 other sRNAs that proved to be sporulation-controlled, but still await the identification of their targets (5). Furthermore, in addition to the well-studied RNAIII from *Staphylococcus aureus* (6), 12 novel sRNAs from *Staphylococcus aureus* pathogenicity islands have been detected (7) as well as three Hfq-binding sRNAs of *Listeria monocytogenes* with still unknown function (8), and nine novel sRNAs from *Listeria monocytogenes* within intergenic regions found by *in silico*-based approaches (9). Additionally, more than 100 potential 6S RNA species have been identified by bioinformatics approaches, and many of them were verified experimentally, among them two 6S RNA species in *B. subtilis* (10,11). Still, the identification of mRNA targets of the recently discovered sRNAs is a challenging issue, and has been successful only in less than one-third of all cases.

One important hallmark of many trans-encoded regulatory RNAs from *E. coli* is their ability to bind the Sm-like abundant RNA chaperone Hfq (12). While several sRNAs have been found to require Hfq for their stability, some were shown to need Hfq for efficient complex formation with their target RNA (13,14). For DsrA/*rpoS*/Hfq, the pathway of complex formation has been investigated by biophysical techniques (15). However, for sRNAs from Gram-positive bacteria, the putative function of Hfq is still elusive. At least in one case, staphylococcal RNAIII/*spa* interaction, no influence of Hfq has been found (16).

In contrast to the *cis*-encoded sRNAs from accessory genetic elements like plasmids, phages, transposons that have been studied in detail over the past 25 years [reviewed in (17)], relatively little is known about structural requirements, binding kinetics and mechanisms or degradation pathways of these new trans-encoded regulatory sRNAs. Although complexes between sRNA and mRNA

*To whom correspondence should be addressed. Tel: +49 3641 949570/571; Email: Sabine.Brantl@rz.uni-jena.de

have been detected *in vitro* in some instances, only in five cases secondary structures of such complexes predicted by Mfold have been confirmed by experimental secondary structure probing. These include MicF/*ompF* (18), Spot42/*galK* (19), RyhB/*sodB* (20), MicA/*ompA* (14,21) from *E. coli* and RNAIII/*spa* from *Staphylococcus aureus* (22). So far, the region of initial contact between a trans-encoded sRNA and a target RNA sharing more than one complementary region has not been narrowed down. The mechanism of action has been proposed in some cases, but not always corroborated by a combination of *in vivo* and *in vitro* experiments.

The 205-nt untranslated RNA SR1 from the *B. subtilis* genome was found in our group by a combination of computer predictions and northern blotting (23). Recently, we have shown that SR1 is a *bona fide* antisense RNA that acts by basepairing with its primary target, *ahrC* mRNA, the transcriptional activator of the *rocABC* and *rocDEF* arginine catabolic operons (24). *In vitro* translation data and translational reporter gene fusions suggested that SR1 might inhibit *ahrC* translation at a post-initiation stage. Hfq was shown to be dispensable for the stability of SR1.

Here, we provide a detailed *in vitro* characterization of SR1 and the SR1/*ahrC* complex with and without Hfq. We determined the region of initial contact between SR1 and *ahrC*. Furthermore, a combination of toeprinting and SR1/*ahrC* complex probing studies demonstrated that SR1 inhibits translation initiation of *ahrC* mRNA by inducing structural changes between the *ahrC* SD sequence and the first complementary region G. In contrast to many *E. coli* sense/antisense systems, Hfq was shown to be exclusively required for translation of *ahrC* RNA, but not for promoting the SR1/*ahrC* interaction. The intracellular concentration of SR1 in *B. subtilis* was calculated to be 30 nM in log phase and 315 nM in stationary phase in complex TY medium.

MATERIALS AND METHODS

Enzymes and chemicals

Chemicals used were of the highest purity available. *Taq* DNA polymerase was purchased from Roche or SphaeroQ, Netherlands, respectively, RNA ligase from New England Biolabs and Thermoscript reverse transcriptase and M-MuLV reverse transcriptase from Invitrogene and Fermentas, respectively. Firepol polymerase was purchased from Solis Biodyne, Estonia.

Strains, media and growth conditions

Escherichia coli strains DH10B and ER2566(Δ*hfq::kan*) were used for cloning and for expression of the *B. subtilis hfq* gene, respectively. *Bacillus subtilis* strains DB104 (25) and *E. coli* strains were grown in complex TY medium (24).

In vitro transcription and secondary structure analysis of SR1, ahrC and SR1/ahrC complexes

In vitro transcription and partial digestions of *in vitro* synthesized, 5′-end-labelled SR1 and *ahrC* RNA species with ribonucleases T1, T2 and V were carried out as described (26). For the analysis of SR1/*ahrC* complexes with T1, T2 and V, either SR1 or *ahrC* were 5′ end-labelled and a 6- to 60-fold excess of the cold complementary RNA was added prior to RNase digestion.

Analysis of RNA–RNA complex formation

Both *ahrC* RNA and SR1 were synthesized *in vitro* from PCR-generated template fragments with primer pairs indicated in Table 1 Supplementary Data. SR1/*ahrC* complex formation studies were performed as described previously (24). Complex formation in the presence of Hfq was assayed in TMN buffer (24) using purified Hfq from *B. subtilis*.

Purification of *B. subtilis* Hfq

For the purification of *B. subtilis* Hfq, the IMPACT™-CN system from New England Biolabs was used. To prevent the purification of *E. coli*/*B. subtilis* Hfq-heterohexamers, *E. coli* strain ER2566(*hfq::kan*) was transformed with plasmid pTYB11-BsHfq. (All plasmids used in this study are summarized in Table 1). The resulting strain was grown at 37°C till $OD_{560} = 0.7$, induced with 0.25 mM IPTG, and grown at 18°C for further 18 h. The fusion protein was purified by affinity chromatography on a chitin column as described by the manufacturer. On-column cleavage was performed with 20 mM Tris-HCl pH 8.0, 500 mM NaCl and 50 mM DTT for 20 h at room temperature. Millipore microcon columns were used to concentrate the eluted Hfq protein and to exchange the buffer for 50 mM Tris-HCl pH 8.0. The purified protein was stored at 4°C.

Construction of plasmids for the *in vivo* reporter gene test system

For the construction of the three translational fusions, chromosomal DNA from *B. subtilis* DB104 was used as

Table 1. Plasmids used in this study

Plasmid	Description	Reference
pTYB11-BsHfq	pTYB11 vector with *B. subtilis hfq* gene	P. Valentin-Hansen
pGF-BgaB	Integration vector for *amyE* gene, heat-stable β-galactosidase from *B. stearothermophilus* without SD for translational fusions, Km^R, Ap^R	27
pGGA4	pGF-BgaB with nt 1 to 119 of *ahrC*	this study
pGGA6	pGF-BgaB with nt 1 to 113 *ahrC*	this study
pGGA7	pGF-BgaB with nt 1 to 279 of *ahrC* but lacking nt 102–112	this study
pGGA8	pGF-BgaB with nt 1 to 119 of *ahrC*, but 2 nt exchange	this study

template in three PCR reactions with upstream primer SB979 and the corresponding downstream primers SB980 (pGGA4), SB987 (pGGA6) and SB1065 (pGGA8). All fragments were digested with BamHI and EcoRI and inserted into the BamHI/EcoRI vector pGF-BgaB (27) encoding the promoterless heat-stable β-galactosidase from *B. stearothermophilus*. For the construction of plasmid pGGA7 carrying an internal deletion of 11 bp (nt 102 to 112) of *ahrC*, a two-step PCR with outer primers SB979 and SB976 and internal primers SB989 and SB988 was performed on chromosomal DNA as template, the third PCR product obtained with SB979 and SB976 cleaved with BamHI and EcoRI and inserted into the BamHI/EcoRI vector pGF-BgaB.

Toeprinting analysis

The toeprinting assays were carried out using 30S ribosomal subunits, $ahrC_{483}$ mRNA and $tRNA^{fMet}$ basically according to (28). The 30S ribosomal subunits devoid of initiation factors were prepared from *E. coli* strain MRE600 essentially as described by Spedding (29). The 5′-[^{32}P]labelled *ahrC*-specific oligonucleotide SB1068 (5′ TAC CGT GGC CTG CGT TAC) complementary to *ahrC* mRNA was used as a primer for cDNA synthesis in the toeprinting reactions. An aliquot of 0.04 pmol of *ahrC* mRNA annealed to primer SB1068 was incubated at 37°C without or with 0.4 pmol of 30S subunits and 8 pmol of uncharged $tRNA^{fMet}$ (Sigma) before supplementing with 1 µl M-MuLV-RT (80 units). cDNA synthesis was performed at 37°C. Reactions were stopped after 10 min by adding formamide loading dye. The samples were separated on a denaturing 8% polyacrylamide gel. For the analysis of the effect of sRNAs on 30S complex formation, $ahrC_{483}$ mRNA and the corresponding sRNA were incubated for 15 min at 37°C before the addition of 30S ribosomes and initiator tRNA. Toeprint efficiency was determined by PhosphorImaging using the Image-quant software package (PC-BAS 2.0).

Preparation of total RNA and northern blotting

Preparation of total RNA and northern blotting were carried out as described previously (23).

RESULTS

Secondary structures of SR1 and truncated SR1 species

So far, only for a few chromosomally encoded regulatory sRNAs, secondary structures have been determined experimentally. Examples include MicF (18), OxyS (30), RNAIII of *S. aureus* (31), DsrA (32), Spot42 (19), RyhB (20) and MicA (14,21). Since computer-predicted RNA structures often deviate from experimentally determined ones [e.g. RNAIII of pIP501 (33) or RNAI/RNAII of pT181 (34)], we performed limited digestions with structure-specific ribonucleases *in vitro* to determine the secondary structure of SR1. The wild-type SR1 (205 nt) as well as the 3′ truncated species $SR1_{132}$, the 5′ truncated species $SR1_{98}$ and the 5′ and 3′ truncated species $SR1_{78}$ were 5′-end labelled, gel-purified and treated with RNases T1 (cleaves 3′ of unpaired G residues), T2 (unpaired nucleotides with a slight preference for A residues) and V1 (double-stranded or stacked regions). Figure 1A shows an analysis of $SR1_{205}$ and the truncated species $SR1_{132}$

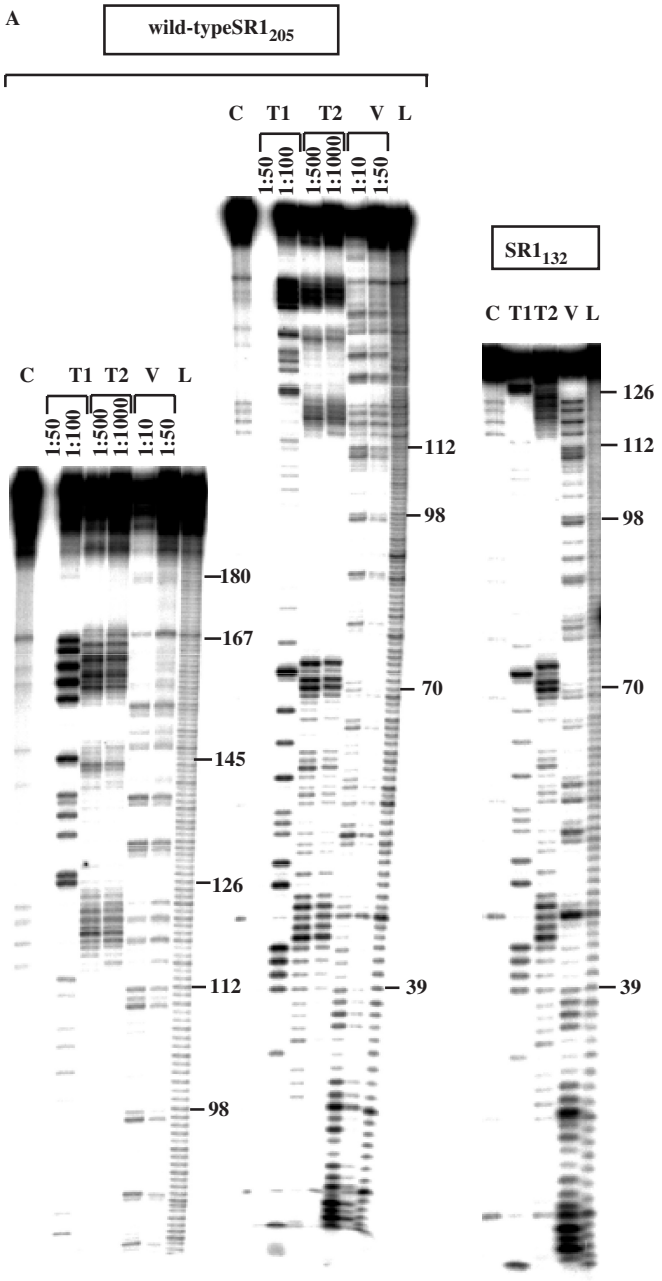

Figure 1. Secondary structures of SR1 species of different lengths. (**A**) Secondary structure probing of wild-type SR1 (205 nt) and truncated species $SR1_{132}$ with RNases. Purified, 5′ end-labelled SR1 was subjected to limited cleavage with the RNases indicated. The digested RNAs were separated on 8% denaturing gels. Autoradiograms are shown. RNase concentrations used were: T1: 10^{-2} U/µl (1:50), T2: 10^{-1} U/µl (1:500), V1: 10^{-1} U/µl (1:10), C, control without RNase treatment, L, alkaline ladder. (**B**) Proposed secondary structure of SR1. A structure consistent with the cleavage data in Figure 1A and additional experiments (data not shown) is depicted. Major and minor cuts are indicated by symbols (see box). The three main stem-loops SL1, SL2 and SL3 are indicated.

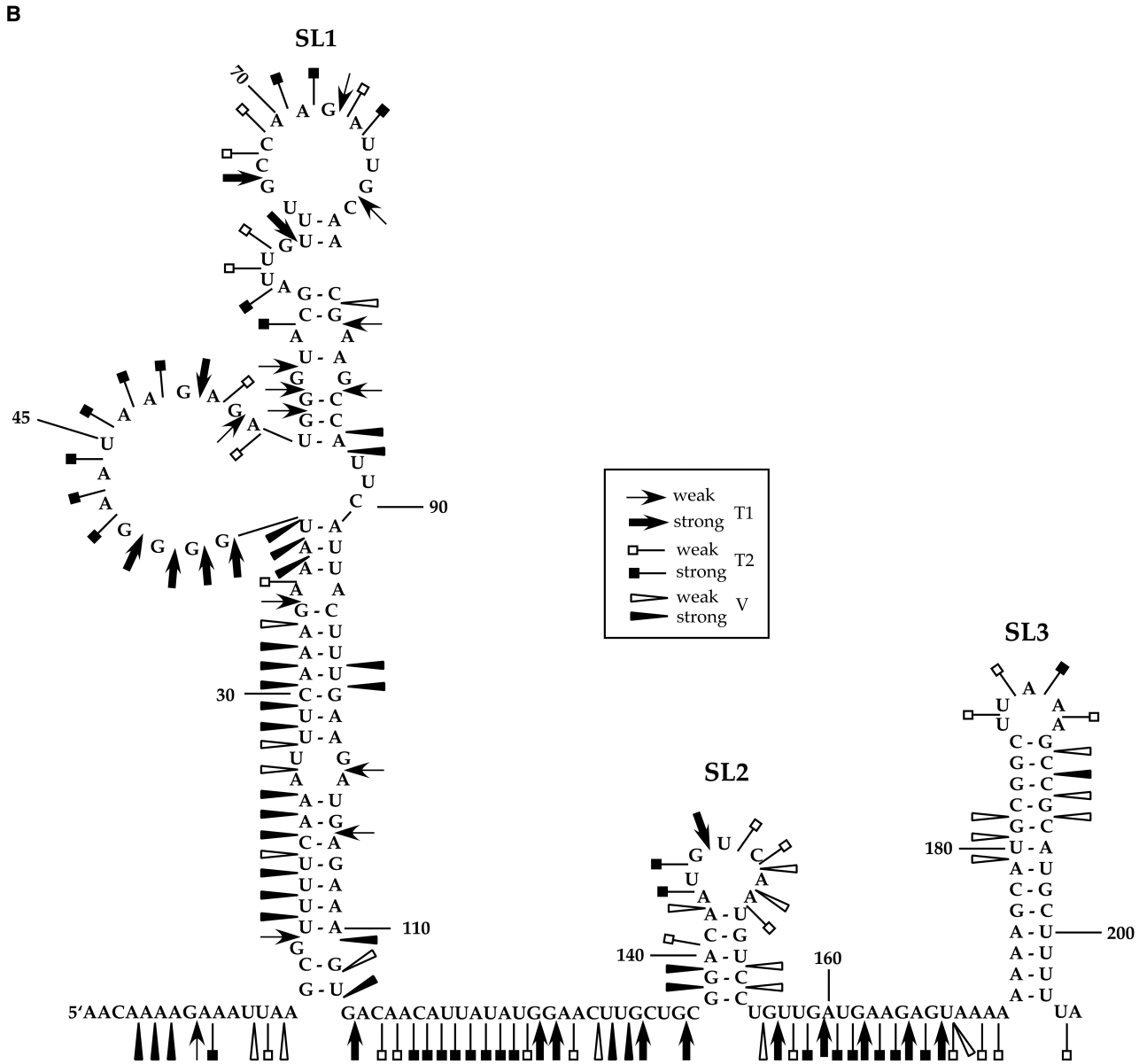

Figure 1. Continued.

whereas Figure 2B contains the schematic representation of the structure of $SR1_{205}$ derived from the cleavage data. The experimentally determined structure for wild-type SR1 comprises three main stem-loops: SL1 (nt 1 to 112), SL2 (nt 138 to 154) and the terminator stem-loop SL3 (nt 173 to 203) interrupted by two single-stranded regions SSR1 (nt 113 to 137) and SSR2 (nt 155 to 172). It deviates from the structure predicted with Mfold in the 5′ as well as in the 3′ portion: The 5′ part was found to be single-stranded between nt 38 and 51, and the double-stranded stem proved to be much longer than predicted and comprises 20 paired nucleotides (nt) interrupted by three internal loops or bulged-out bases, respectively, compared to only 10 paired nt in the predicted structure. For the 3′ part, two stem-loops and the terminator stem-loop were predicted by Mfold, whereas the structure probing data support in addition to the terminator stem-loop only the second stem-loop SL2 in the centre of a long single-stranded region.

Structure probing of the 5′ 132 nt of SR1 (Figure 1A, right part) showed that this portion of the molecule folded independently and exactly as in the full-length sRNA. The secondary structure for the 3′ 98 nt of SR1 contained exactly the terminator stem-loop as in wild-type SR1 (not shown) and the secondary structure for $SR1_{78}$ comprising nt 109 to 186 revealed the single stem-loop SL2 surrounded by single-stranded regions as expected (not shown).

The information on the secondary structures of the truncated derivatives was necessary to assess the data on complex formation between different SR1 species and its target, *ahrC* mRNA.

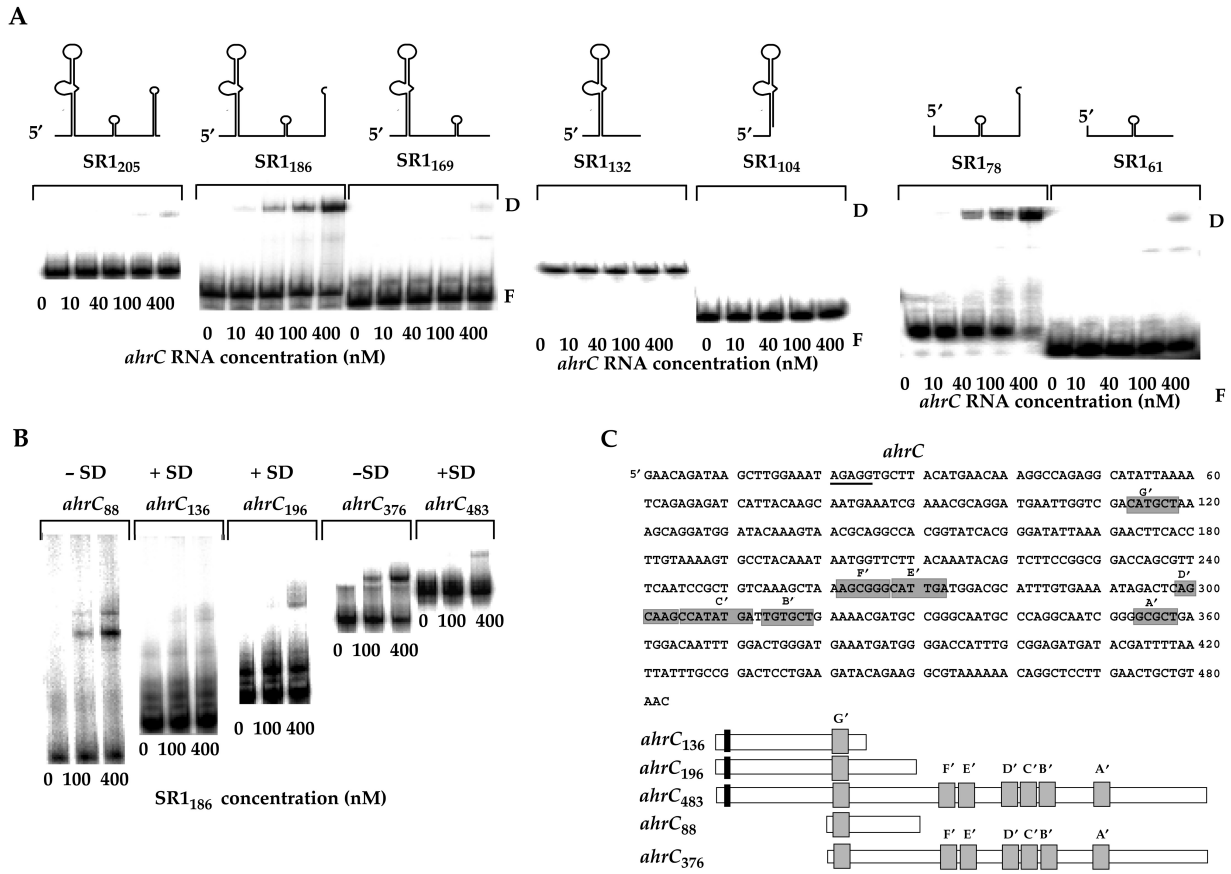

Figure 2. Binding assays of wild-type and truncated SR1/*ahrC* RNA pairs. Binding experiments were performed as described in Materials and Methods section. Autoradiograms of gel-shift assays are shown. The concentration of unlabelled *ahrC* RNA species or SR1 species is indicated. F, labelled RNA, D duplex between SR1 and *ahrC* RNA. (**A**) Binding assays with wild-type and truncated SR1 derivatives. SR1 species were 5′ end-labelled with [γ^{32}P]-ATP and used in at least 10-fold lower equimolar amounts compared to the targets. $ahrC_{376}$ comprising the 3′ part of *ahrC* mRNA with nt 113 to 483 was used in all cases. Above, the schematic representation of the SR1 species is shown. (**B**) Binding assays with wild-type and truncated *ahrC* species. *ahrC* RNA species were 5′ end-labelled with [γ^{32}P]-ATP and used in at least 10-fold lower equimolar amounts compared to $SR1_{186}$. (**C**) Overview on the *ahrC* mRNA species used in this work. The sequence of the *ahrC* gene is shown. Regions A′ to G′ complementary to SR1 are indicated by grey boxes, the SD sequence is underlined. Start and stop codon are shown in Italics. Below, a schematic representation of the 5 *ahrC*-mRNA species used in this work is shown. Black rectangle, SD sequence. grey boxes, regions complementary to SR1.

Binding assays of truncated SR1/*ahrC* mRNA pairs

Previously, we have shown that SR1 binds to the 376 3′ nt of *ahrC* mRNA ($ahrC_{376}$, Figure 2C) with an equilibrium dissociation rate constant K_D of 3.21×10^{-7} M (24). Since seven regions of complementarity have been predicted between SR1 and *ahrC* mRNA [(24) and Figure 2C], we intended to narrow down the segment of SR1 that is required for the initial contact with its target. To this end, SR1 species of different lengths were generated by *in vitro* transcription with T7 RNA polymerase, 5′ end-labelled, gel-purified and used for binding assays with the $ahrC_{376}$ RNA. The results are shown in Figure 2A: 3′ truncated SR1 derivatives $SR1_{132}$ and $SR1_{104}$ comprising only stem-loop SL1 and lacking SL2 and the terminator stem-loop, were not able to form complexes with *ahrC* mRNA even at 400 nM. In contrast, 5′ truncated species $SR1_{78}$ comprising only the single-stranded region, SL2 and the 5′ half of the terminator stem-loop, was as efficient in complex formation as $SR1_{186}$, a species that only lacked the 3′ half of the terminator stem-loop, but otherwise contained the complete wild-type sequences and structures. In accordance with these data, both $SR1_{169}$ lacking SL3 completely and $SR1_{61}$, lacking SL1 and SL3, were significantly impaired in the interaction with their target and only at 400 nM *ahrC* mRNA, a weak complex was observed.

From these results we can conclude that for efficient complex formation between SR1 and *ahrC* mRNA, SL1 and the 3′ half of SL3 are not required. Furthermore, the opening of the terminator stem-loop SL3 seems to be essential for an efficient interaction and a sequence located in the 5′ half of SL3 proved to be important for the contact between antisense-RNA and target.

To analyse the regions of *ahrC* required for efficient pairing with SR1, five 5′ labelled *ahrC* RNA species (shown schematically in Figure 2C) were used in complex formation experiments with $SR1_{186}$ (Figure 2B). As expected, labelled $ahrC_{376}$ comprising nt 108 to 483 of *ahrC* RNA, but lacking the 5′ part and the SD sequence of

ahrC formed a complex with unlabelled $SR1_{186}$ with the same K_D as determined previously for the labelled SR1/unlabelled $ahrC_{376}$ pair. The same efficiency for complex formation was observed for $ahrC_{88}$ containing region G′ but lacking the SD sequence. By contrast, labelled $ahrC_{136}$ and $ahrC_{196}$ comprising the 5′ 136 and 196 nt of *ahrC* mRNA, respectively, including SD sequence and region G′, were significantly impaired in complex formation with unlabelled $SR1_{186}$. The complete $ahrC_{483}$ mRNA including 5′ end, SD and all complementary regions to SR1 formed a weak complex with SR1 only at 400 nM concentration. These results suggest that the SD sequence of *ahrC* mRNA might be sequestered by intramolecular basepairing and that a factor might be needed to facilitate ribosome binding.

Secondary structure of the SR1/*ahrC* complex

The results from the binding assays indicate that $SR1_{78}$ is sufficient for efficient complex formation with *ahrC* mRNA and that without opening of the 5′ half of the terminator stem-loop no efficient complex can form. To investigate the alterations in the secondary structures of SR1 and *ahrC* upon pairing, the secondary structure of the $SR1_{186}/ahrC_{376}$ complex was determined. To ascertain alterations in the SR1 structure, labelled $SR1_{186}$ was incubated with a 6- to 60-fold excess of unlabelled *ahrC* RNA, the complex was allowed to form for 5 min at 37°C, and, subsequently, partially digested with RNases T1, T2 and V1. In parallel, free $SR1_{186}$ was treated in the same way. Figure 3A shows the result. As expected, no significant alterations were observed within the 5′ 112 nt of SR1 that contain only region A (nt 15 to 19) complementary to *ahrC*. By contrast, significant alterations in the T1, T2 and V cleavage pattern were observed within the other six complementary regions B, C, D, E, F and G (Figure 3A, right half). The data are summarized in Figure 3C: Whereas in region B, only one reduced T1 cut was detected at G_{113}, drastic alterations were observed in both regions C and G: In C, all 9 nt complementary to *ahrC* showed reduced T2 cleavages, G_{126} and G_{127} exhibited reduced T1 cleavage and at U_{123} and U_{125}, an induction of V1 cleavage was detected indicating that this region became double-stranded upon pairing with *ahrC*. The same was true for region G, where the cleavage pattern at all positions was altered compared to free SR1: nt 175 to 181 showed a decreased T2 cleavage, among them G_{176} and G_{181} a reduced T1 cleavage, whereas at U_{180} and G_{181} new V cuts appeared. Fewer changes were found in regions D, E and F, where G_{133} (region D), U_{146} and A_{147} (region E) and G_{156}, U_{157} and U_{158} (region F) were not single-stranded anymore and, instead, U_{132} and U_{133} (region D), A_{148} and A_{149} (region E) as well as U_{155} and G_{156} (region F) showed induced V cleavages, i.e. became double-stranded.

To further substantiate these results, secondary structure probing was performed with a complex formed between labelled *ahrC* and a 6- to 60-fold excess of unlabelled SR1. To corroborate our previous hypothesis that SR1 does not inhibit the translation initiation at the *ahrC* SD sequence, both the complex between $ahrC_{136}$ (5′ 136 nt of *ahrC* including SD sequence and region G′) and the complex between $ahrC_{376}$ (lacking the 5′ 112 nt of *ahrC* including SD, but comprising all regions complementary to SR1) were probed with RNases T1, T2 and V. The results are shown in Figure 3B and are summarized in Figure 3D: In the case of $ahrC_{376}$, induced V cuts were visible in regions E and G. Furthermore, between region E and D and in region C, T2 cuts were induced which is expected when one strand of a double-stranded region interacts with SR1, and the other half becomes, consequently, single-stranded. The same holds true for the induced T1 cuts in region B and the induced T2 cut in the region upstream of B.

The lower part of Figure 3B presenting the results of $SR1/ahrC_{136}$ interaction clearly shows that the *ahrC* SD sequence itself was not affected upon addition of increasing amounts of unlabelled SR1. Surprisingly, a number of alterations could be observed further downstream from it and upstream of complementary region G′. In particular, prominent V cuts were induced at nt 40, nt 46 to 48, nt 52, nt 56, nt 71 and nt 90, accompanied by induced T2 cuts around nt 56 and 74, 75, 77 and 78 (Figure 3B left and Figure 3D). These data suggest that binding of SR1 causes structural changes in the 5′ part of *ahrC* mRNA between the SD sequence and region G′.

The initial contact between SR1 and *ahrC* RNA requires complementary region G

As published previously (24), one out of seven regions of complementarity between SR1 and *ahrC* RNA comprises nt 176 to 181 within the 5′ half of the SR1 terminator stem-loop SL3 (designated G) and nt 113 to 118 of *ahrC* mRNA (designated G′). If these two regions were involved in a first contact between SR1 and *ahrC* RNA, nucleotide exchanges in either SR1 or *ahrC* RNA should impair or abolish complex formation, and compensatory mutations should, at least partially, restore binding. To test this hypothesis, three mutated $SR1_{186}$ species with either a 10 nt exchange (5′AGCAUGCGGC to 5′ UCGUACGCCG) between nt 176 and 185 denoted $SR1_{186\_G10}$, a 6 nt exchange (5′AGCAUG to 5′UCGUAC), denoted $SR1_{186\_G6}$ or a 2 nt exchange ($G_{177}C_{178}$ to $T_{177}T_{178}$) denoted $SR1_{186\_G2}$, were assayed in complex formation with wild-type $ahrC_{88}$ comprising nt 109 to 196 of *ahrC* mRNA (region G′). The 6 and 10 nt exchanges were designed such that the GC/AU content of the region was not altered compared with the wild-type. As shown in Figure 4A, no interaction between these three mutated SR1 species and wild-type *ahrC* RNA was observed. By contrast, the exchange of only C_{178} to G ($SR1_{186\_G1}$) did not impede complex formation, suggesting that either G_{177} is most important for the initial contact or that substitution of one nucleotide is not sufficient to cause an effect. Interestingly, when *ahrC* $RNA_{88\_G'2}$, a derivative of the same length carrying the compensatory mutations to $SR1_{186\_G2}$ was used, binding could be restored (Figure 4A and B) confirming a specific basepairing interaction between SR1 and *ahrC* mRNA. When a longer $ahrC_{376}$ RNA comprising all seven

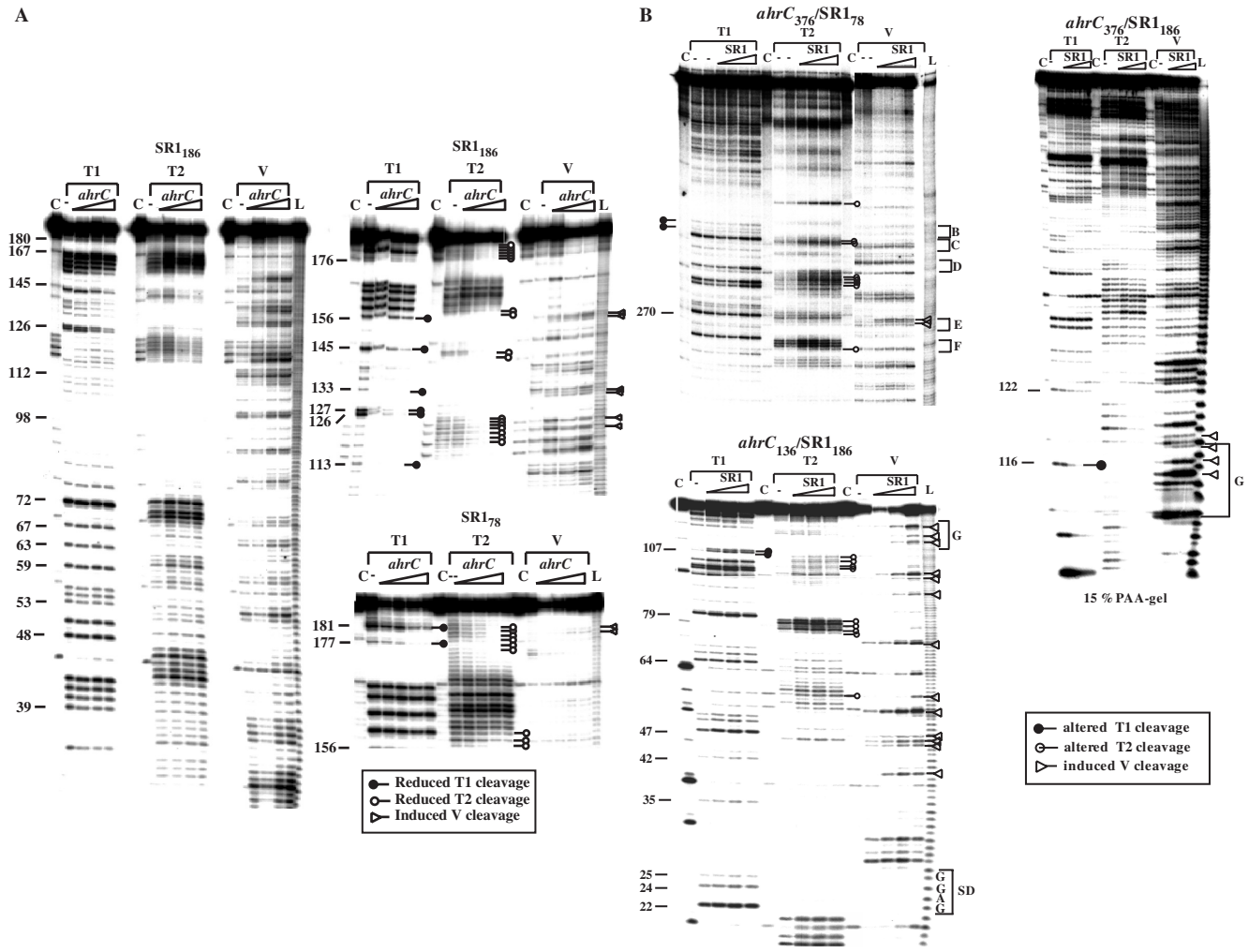

Figure 3. Secondary structure probing of the SR1/*ahrC* complex. (**A**) Alterations in the SR1 secondary structure upon complex formation with *ahrC* mRNA. Purified, 5′ end-labelled $SR1_{186}$ (13 nM) was incubated with increasing amounts of unlabelled $ahrC_{376}$ (80, 200 and 800 nM), complex allowed to form for 5 min at 37°C and subjected to limited cleavage with the RNases indicated. The digested RNAs were separated on 8% denaturing gels. Autoradiograms are shown. RNase concentrations used were: T1: 10^{-2} U/µl, T2: 10^{-1} U/µl, V1: 10^{-1} U/µl C, control without RNase treatment, L, alkaline ladder. Left; entire gel. Right, long run of the same samples allowing a better separation of the complementary regions B, C, D, E and F. Nucleotide positions are included. Altered T1, T2 and V cleavages are indicated by the symbols shown in the box. Right half, below: $SR1_{78}$: For a better resolution of the complex within complementary regions F and G, the secondary structure of the complex between $SR1_{78}$ (6.25 nM) and $ahrC_{376}$ (80, 200, 800 and 1600 nM) was mapped, the same concentrations of T1, T2 and V were used and the products separated by a long run on an 8% gel. (**B**) Alterations in the *ahrC* secondary structure upon complex formation with SR1. Purified, 5′ end-labelled $ahrC_{136}$ or $ahrC_{376}$ (13 nM) was incubated with increasing amounts of unlabelled $SR1_{186}$ (80, 200 and 800 nM), complex formation, cleavage and gel separation were performed as above. (**C**) Schematic representation of the SR1 secondary structure with indicated structural changes upon binding to *ahrC* RNA. Altered T1, T2 and V cleavages are denoted as shown in the box. Regions complementary to *ahrC* RNA are highlighted by grey boxes. (**D**). Schematic representation of the secondary structure of $ahrC_{136}$ and $ahrC_{376}$ with indicated structural changes upon binding to SR1. Altered T1, T2 and V cleavages are denoted as shown in the box. Regions complementary to SR1 are highlighted by grey boxes. Nucleotide numbering for both RNAs is as in Figure 2.

complementary regions G′ to A′ was analysed, binding was abolished by the above-mentioned mutations too, and partially restored with the compensatory mutation $ahrC_{376\_G'2}$ mRNA (not shown). These data indicate that the complementary region G of SR1 (nt 176 to 181) plays an important role for the recognition of *ahrC* mRNA.

To investigate the contribution of the other regions of SR1 complementary to *ahrC* RNA to efficient binding with its target, two $SR1_{186}$ species carrying 9 nt exchanges each in either region C (nt 119 to 127)—$SR1_{S5}$—or region E and the first 2 nt of region F (comprising nt 146 to 154)—$SR1_{S6}$—were analysed for complex formation with *ahrC* RNA carrying the wild-type or mutated regions (Figure 4C). Complex formation was significantly impaired in both cases: $SR1_{S5}$ exhibited about 10-fold and $SR1_{S6}$ about 30-fold decreased efficiency to pair with *ahrC* RNA. A combined substitution of regions C, E and 5′ F ($SR1_{S7}$) or a combined exchange of regions C, D, E and 5′ F ($SR1S_9$) resulted in a complete loss of pairing. Figure 4D shows a schematic representation of the four mutated $SR1_{186}$ species.

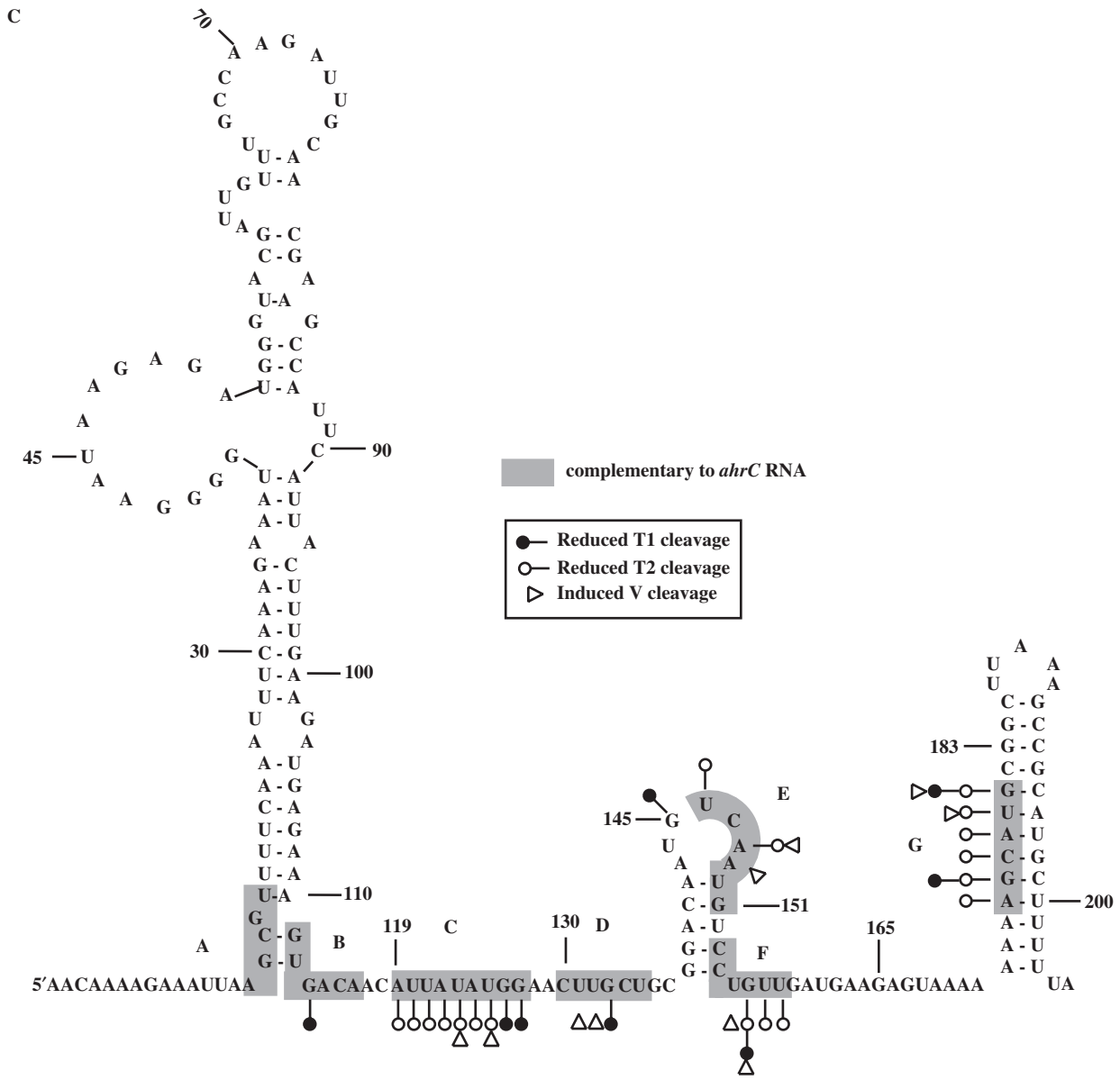

Figure 3. Continued.

These data indicate that, although region G is crucial, regions C, D, E and F contribute to efficient pairing.

An *in vivo* reporter gene test system confirmed the importance of region G for the interaction between SR1 and *ahrC* mRNA

To test the importance of region G′ (nt 113 to 118 of *ahrC*-mRNA complementary to nt 176–181 of SR1) for the interaction with SR1 *in vivo* in *B. subtilis*, the following three translational *ahrC-BgaB* fusions were constructed: pGGA6 containing nt 1 to 113 but lacking all but one nt of region G, pGGA4 comprising nt 1 to 119, i.e. the entire region G + one additional nt, and, hence, no other complementary region, and pGGA7 identical to pGGA3 (comprising G, F and E, 24) but lacking nt 102 to 112 upstream of G. All fusions were integrated into the *amyE* locus of the *B. subtilis* DB104 chromosome, grown till $OD_{560} \sim 5$ (maximal expression of SR1) and β-galactosidase activities measured. As shown in Table 2, β-galactosidase activities measured with pGGA4 and pGGA7 were, in both cases, about 30-fold lower than that of the pGGA6-integration strain lacking any complementary region to SR1. Since pGGA4 yielded the same decrease in β-galactosidase activity compared to a construct lacking any complementarity with SR1 as our previous construct pGGA3 that encompassed regions G, E and F, it can be concluded that region G alone is sufficient to inhibit *ahrC* translation almost completely. The results obtained with pGGA7 and pGGA4 exclude the possibility that the sequences immediately adjacent to region G are involved in the observed decrease of β-galactosidase activity, e.g. by providing a cleavage site for an RNase.

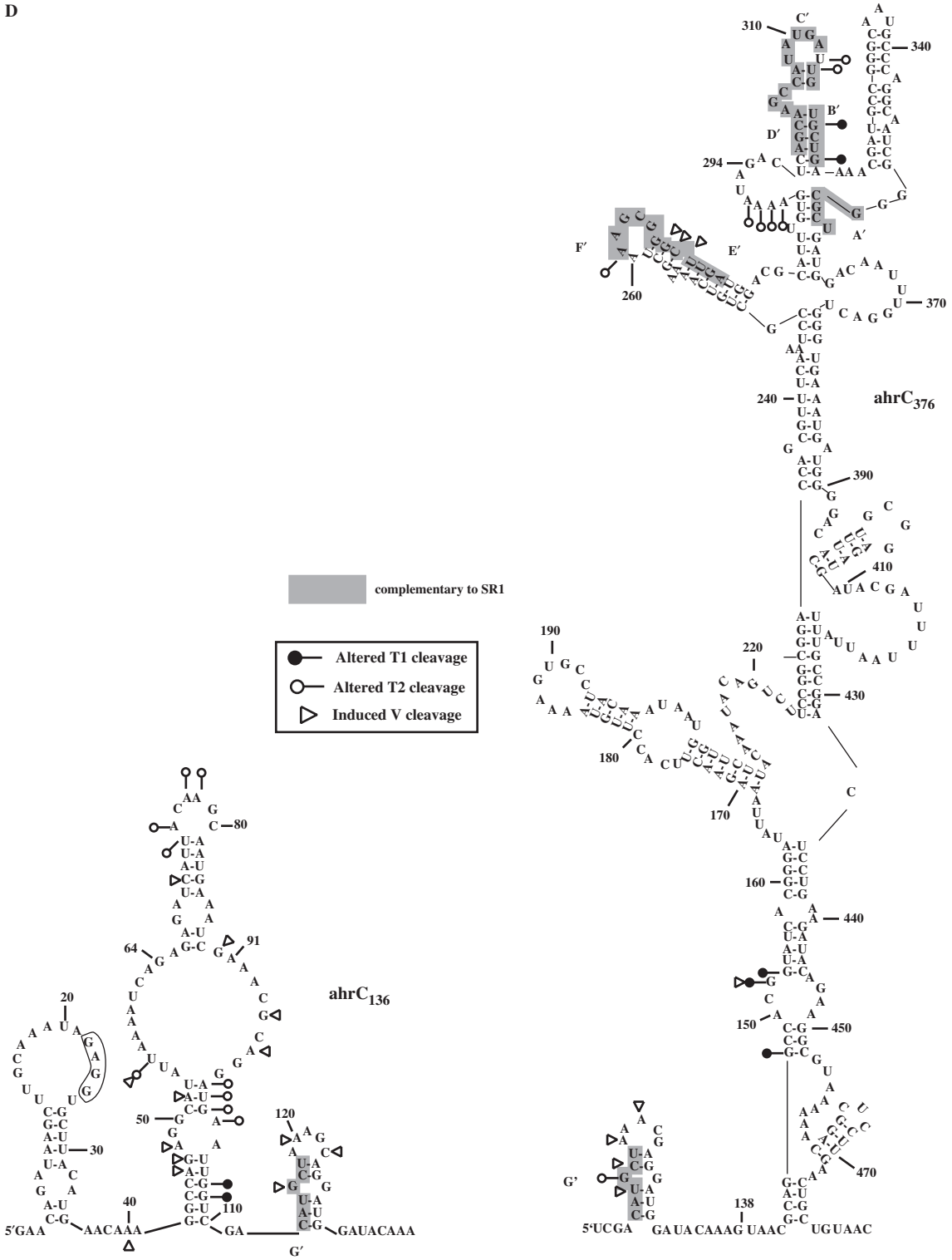

Figure 3. Continued.

To test whether point mutations in region G′ abolish the effect of SR1 on *ahrC* translation, pGGA8 was constructed carrying the same 2 nt exchange as $SR1_{186\_G\text{-}2}$ analysed in the binding assay (Figure 4A), but lacking any sequences downstream from nt 118 (3′ end of region G′) and integrated into the *amyE* locus of *B. subtilis*. The β-galactosidase activity measured with pGGA8 was nearly the same as with pGGA6 (Table 2), confirming the *in vitro* result that the 2-nt exchange in region G prevented the interaction between SR1 and *ahrC*.

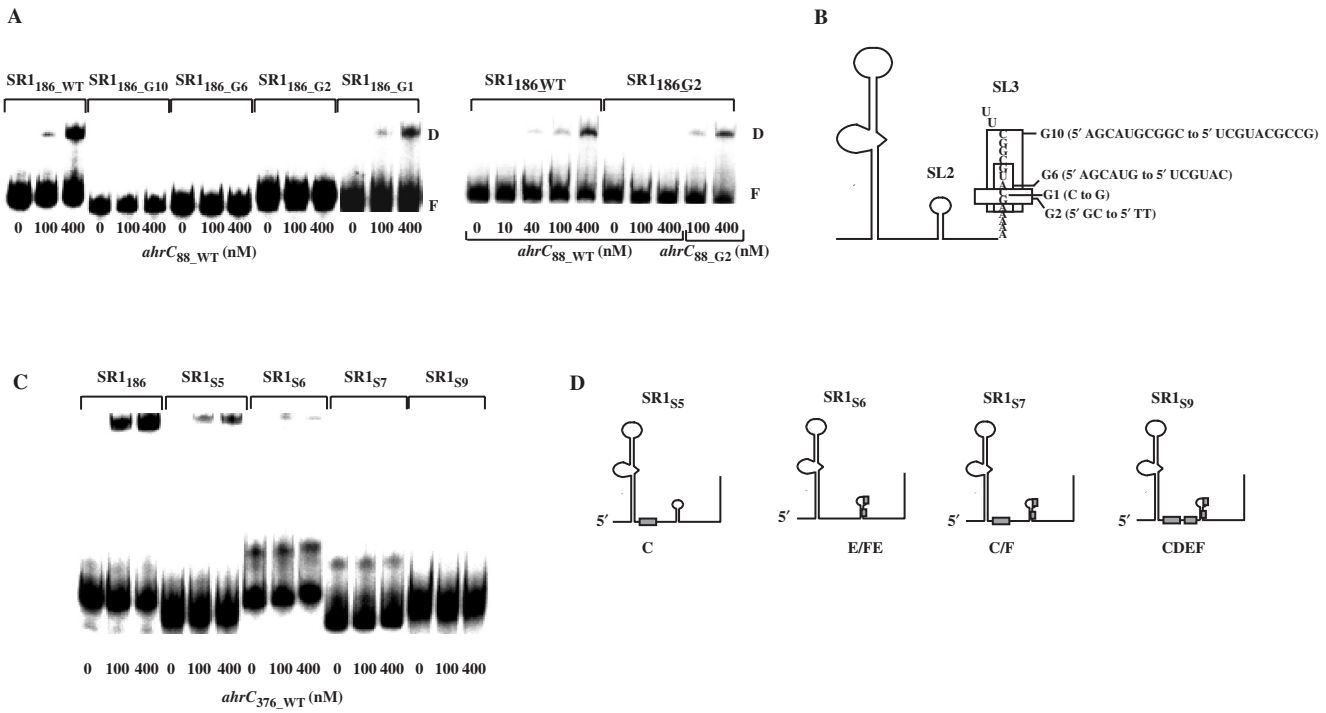

Figure 4. Binding assays of wild-type and mutated SR1/*ahrC* pairs. Binding experiments were performed as described in the Materials and Methods section. Autoradiograms of gel-shift assays are shown. The concentration of unlabelled $ahrC_{88}$ RNA species is indicated. SR1 derivatives were 5′ end-labelled with [γ ^{32}P]-ATP and used in at least 10-fold lower equimolar amounts compared to the targets. F, free SR1, D duplex between SR1 and *ahrC* RNA. (**A**) Analysis of mutations in region G. (**B**) Schematic representation of SR1 with the mutations introduced into region G. (**C**) Analysis of mutations in regions C, D, E and F. (**D**) Schematic representation of the mutated SR1 species. Grey boxes denote the substituted regions.

Hfq does not promote the interaction between SR1 and *ahrC* mRNA, but is required for the translation of *ahrC* mRNA

Many small RNAs from *E. coli* need Hfq for either stability or their interaction with their targets (see Introduction section). Previously, we have shown that Hfq is neither required for the stabilization of SR1 nor that of *ahrC* (24). However, in the absence of Hfq, but presence of SR1, the expression of the downstream SR1 targets, *rocABC* mRNA and *rocDEF* mRNA, was about 3- and 6-fold, respectively, increased. Therefore, we wanted to investigate, whether Hfq is required for the promotion of complex formation with *ahrC* RNA.

To investigate whether Hfq binds SR1, different concentrations of purified *B. subtilis* Hfq were added to labelled wild-type SR1 and two 3′ truncated species $SR1_{186}$ and $SR1_{104}$, and a gel-shift assay was performed. As shown in Figure 5A, all three SR1 species bound Hfq at concentrations of 3–10 μM. To analyse binding of Hfq to *ahrC* RNA, full-length and truncated *ahrC* species were assayed for Hfq binding: As shown in Figure 5B, $ahrC_{136}$, $ahrC_{196}$ and $ahrC_{483}$ (full length) that contain the SD sequence, bound Hfq very efficiently. By contrast, $ahrC_{376}$ lacking the SD sequence bound Hfq less efficiently than $ahrC_{483}$.

Since both SR1 and *ahrC* RNA bound Hfq, we analysed whether Hfq is able to promote the complex formation between both RNAs *in vitro*. For this purpose, purified *B. subtilis* Hfq was added to a final concentration of 10 μM (amount required to bind 50% SR1), to the mixture of 1.0 nM labelled SR1 and different amounts of unlabelled *ahrC* mRNA, incubated for 15 min at 37°C and complexes were separated on 6% native PAA gels. Although a ternary SR1/*ahrC*/Hfq complex formed, this complex was not observed at lower *ahrC* concentrations compared to the binary SR1/*ahrC* complex, and the amount of this complex did not increase with increasing

Table 2. β-Galactosidase activities

Strain	5′ *ahrC* Sequence	β-Galactosidase activity (Miller units)
DB104::pGGA6	113 nt (no)	251 ± 28
DB104::pGGA4	119 nt (G)	7.6 ± 2
DB104:: pGGA7	280 nt (G, F, E, but Δnt102–112)	3.5 ± 1.4
DB104:: pGGA8	119 nt (G, but 2 nt exchange)	240 ± 35
DB104::pGF-BgaB	no	2.9 ± 0.5
DB104::pGGA6 (Δ*hfq::cat*)	113 nt (no)	1.3 ± 0.5

All values represent averages of at least three independent determinations. Plasmid pGF-BgaB is the empty vector. All plasmids contain *ahrC s*equences fused in frame to the promoterless, SD less *gaB* gene encoding the heat-stable β-galactosidase of *B. stearothermophilus* and were inserted into the *amyE* locus of the *B. subtilis* chromosome. β-Galactosidase activities were measured at 55°C. In brackets, the presence of complementary regions to SR1 is denoted.

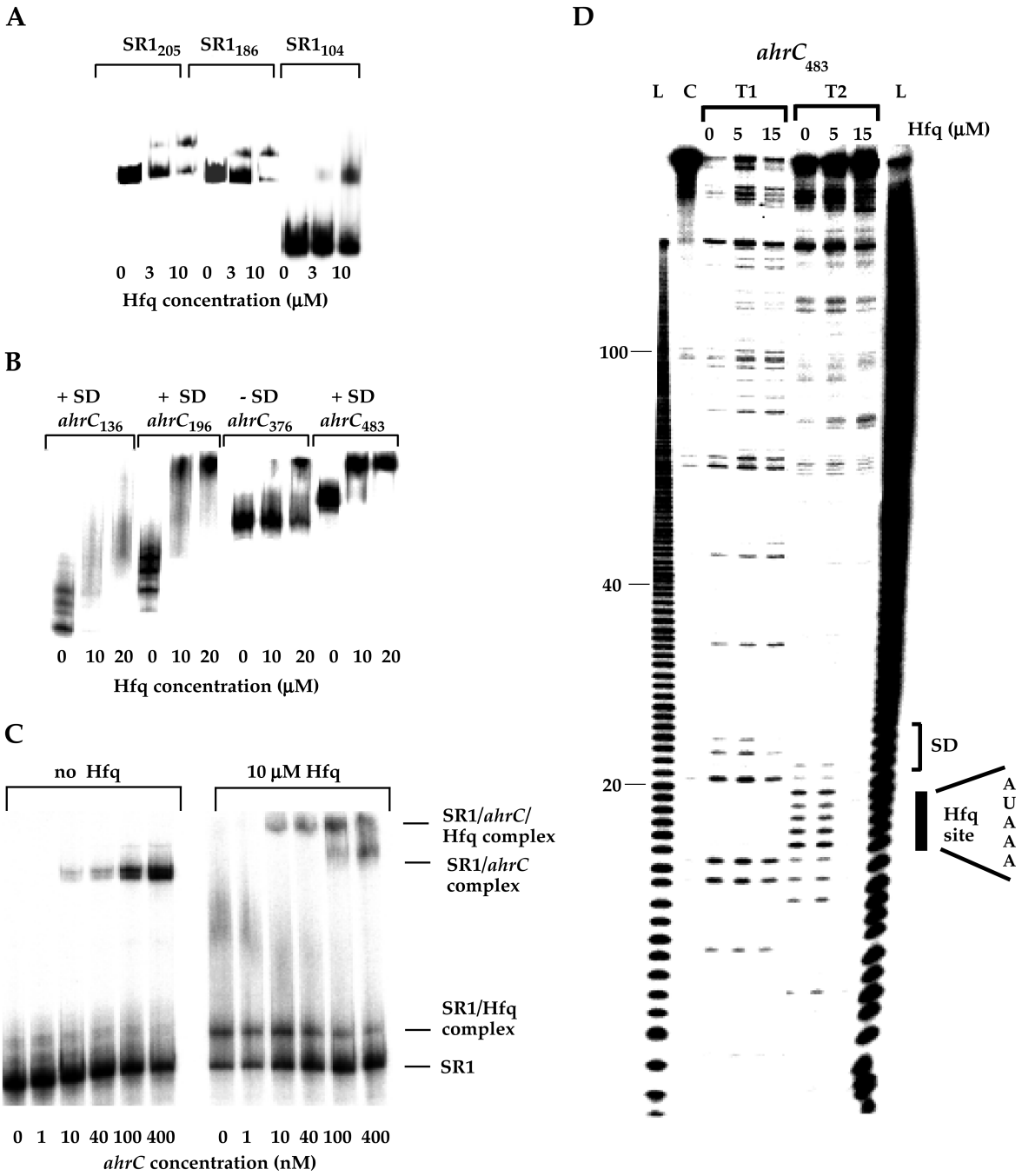

Figure 5. Analysis of the role of Hfq. (**A**). Interaction between SR1 and Hfq. Purified *B. subtilis* Hfq was added to final concentrations as indicated to three SR1 species of different lengths comprising the 205, 186 or 104 nt of 5′ part of wild-type SR1 and binding was assayed as described in the Materials and Methods section. (**B**). Interaction between *ahrC* RNA and Hfq. Purified *B. subtilis* Hfq was added to final concentrations as indicated to four *ahrC* species of different length (see Figure 2C) and binding was assayed as in (A). (**C**). Complex formation between SR1 and *ahrC* RNA in the absence and presence of purified *B. subtilis* Hfq. The interaction between SR1 (final concentration: 1.0 nM) and *ahrC* RNA was assayed in the absence or presence of 10 μM Hfq as described in the Materials and Methods section. The SR1/Hfq complex, the SR1/*ahrC* complex and the ternary SR1/*ahrC*/Hfq complex are indicated. (**D**). Mapping of the Hfq-binding site on *ahrC* mRNA. Purified, 5′ end-labelled $ahrC_{483}$ RNA (13 nM) was incubated for 15 min at 37°C with increasing amounts of Hfq and subsequently subjected to limited cleavage with the RNases T1 and T2 followed by separation on an 8% denaturing polyacrylamide gel. The autoradiogram is shown. RNase concentrations used were as in Figure 1. C, control without RNase treatment, L, alkaline ladder. The Hfq-binding site is indicated by a black bar.

concentrations of unlabelled *ahrC* RNA (Figure 5C). In contrast, upon higher concentrations of unlabelled *ahrC* RNA (≥100 nM), this RNA, apparently, successfully competed with SR1 for Hfq binding, so that the amount of unbound labelled SR1 increased again (Figure 5C). In summary, all these data clearly prove that the RNA chaperone Hfq does not facilitate the interaction between SR1 and its target *ahrC* mRNA.

To reconcile these observations as well as the lacking effect of Hfq on SR1 stability with the increase of the *rocABC* and *rocDEF* mRNA levels in the *hfq* knockout strain, we tested whether the translation of *ahrC* is affected by Hfq. For this purpose, the *ahrC-Bgab* translational fusion pGGA6 was integrated into the *amyE* locus of DB104(Δ*hfq::cat*), and β-galactosidase activity was measured and compared to that determined in the presence of Hfq in DB104. A 250-fold lower β-galactosidase activity was detected in the absence of Hfq, indicating that this RNA chaperone is required for efficient translation of *ahrC* mRNA *in vivo* (Table 2).

To substantiate the role of Hfq in promoting translation of *ahrC* mRNA, the secondary structures of *ahrC* mRNA and SR1 were probed with RNases T1 and T2 in the presence and absence of Hfq. As shown in Figure 5D, one binding site of Hfq on *ahrC* mRNA (5′ AAAUA) is located immediately upstream of the SD sequence. The same assay was used to determine the binding site(s) of Hfq on SR1. Here, one binding site around nt 9–13 in the 5′ part of SR1 and a second in the bulge of stem-loop SL1 (nt 43 to 47) were found (gel not shown). The facts that Hfq gel-shifts with wild-type SR1 and $SR1_{104}$ comprising only the 5′ stem-loop were identical (Figure 5A), support the absence of Hfq-binding sites on SR1 downstream from nt 104.

SR1 blocks ribosome binding to the *ahrC* mRNA translation initiation region

Although the first complementary region between *ahrC* and SR1 is located 87 nt downstream from the *ahrC* SD sequence, we performed a toeprinting analysis (28) to examine the effect of SR1 on formation of the translation initiation complex at *ahrC* mRNA. Figure 6A shows that in the presence of initiator $tRNA^{fMet}$, 30S ribosomal subunits bind to the *ahrC* translation initiation region and block reverse transcription of a labelled primer, annealed downstream, at the characteristic position +15 (start codon A is +1). This signal provides a measure for the formation of the ternary complex, since it is dependent on both 30S subunits and initiator $tRNA^{fMet}$. Addition of increasing amounts of $SR1_{WT}$ or $SR1_{186}$ prior to addition of 30S subunits and $tRNA^{fMet}$ interfered with ternary complex formation, resulting in a weaker toeprint signal

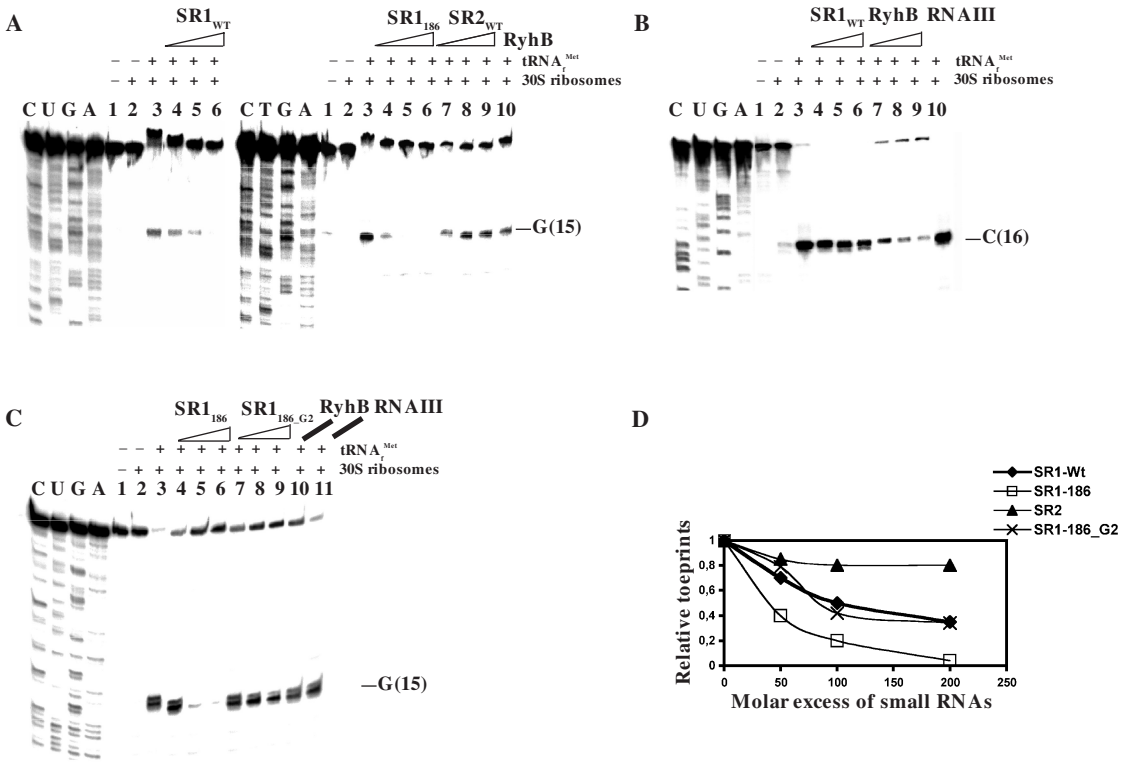

Figure 6. Toeprinting analysis. Ternary complex formation upon addition of different amounts of regulatory RNAs to either $ahrC_{487}$ mRNA or *sodB* mRNA (for details, see the Materials and Methods and Results section). The toeprint signal relative to A of the start codon is marked. Addition of 30S ribosomal subunits and initiator tRNA (lanes 2 and 3) as well as increasing concentrations (50-, 100- and 200-fold excess) of the regulatory RNAs (lanes 4 to 6 and 7 to 9) are indicated above the gels. In all cases, the RNA sequencing reactions (C U G A) were carried out with the same end-labelled oligonucleotide as in the toeprint analysis assays. (**A**) Toeprinting analysis with *ahrC* mRNA. An autoradiogram of ternary complex formation on $ahrC_{487}$ mRNA in the absence or presence of SR1 or heterologous small RNAs (SR2 from *B. subtilis*, RyhB from *E. coli*) is shown. RyhB was added in a 200-fold excess. (**B**) Toeprinting analysis with *sodB* mRNA. An autoradiogram of ternary complex formation on *sodB* mRNA in the absence or presence of SR1 or the cognate small RNA RyhB and the heterologous RNAIII (200-fold excess) from streptococcal plasmid pIP501 is shown. (**C**) Toeprinting analysis of $SR1_{186}$ and $SR1_{186\_G2}$. An autoradiogram of ternary complex formation on $ahrC_{487}$ mRNA in the absence or presence of $SR1_{186}$ or $SR1_{186\_G2}$ carrying a 2-bp substitution in region G is shown. As negative controls, RyhB and RNAIII were added in a 200-fold excess. (**D**) Calculation of the relative toeprints on $ahrC_{487}$ mRNA with three SR1 species and heterologous RNA SR2.

(Figure 6A and C). Thereby, the inhibitory activity of $SR1_{186}$ was higher than that of $SR1_{WT}$ which correlates with its more efficient binding activity to *ahrC* mRNA (Figure 2). By contrast, both the addition of a noncognate small RNA, SR2 from *B. subtilis* or RyhB from *E. coli*, failed to decrease the toeprint signal on *ahrC* mRNA (summarized in Figure 6D) indicating that SR1-dependent inhibition of ribosome binding was specific. To support the specificity of the SR1 inhibitory action on ternary complex formation on *ahrC* mRNA, a control toeprint was performed with SR1 and *sodB* mRNA (target of RyhB). Since SR1 did not affect ternary complex formation on *sodB* mRNA (Figure 6B), whereas RyhB did as expected, it can be excluded that the effect of SR1 on *ahrC* mRNA is simply due to binding to the ribosome. To corroborate the importance of complementary region G for the interaction between SR1 and *ahrC* mRNA, an additional toeprinting assay was carried out with the G-region mutant $SR1_{186\_G2}$ compared to $SR1_{186}$ (Figure 6C). The autoradiogram and the quantification (Figure 6D) show that this mutant is clearly impaired in blocking the binding of the 30S initiation complex, although it has still some residual activity. This result confirms both the specificity of the SR1/ahrC interaction and substantiates our conclusion from the binding assays (Figures 2 and 4) that G is required for the initial contact between SR1 and *ahrC* mRNA. In summary, these data demonstrate that binding of SR1 to *ahrC* mRNA prevents the formation of translation initiation complexes.

The intracellular concentration of SR1 increases about 10-fold in stationary phase

To determine the intracellular concentration of SR1 in *B. subtilis* in logarithmic and stationary growth phase, strain DB104 was grown in complex medium, and samples were withdrawn at OD 2 (log phase) and OD 4.5 (onset of stationary phase). Cell numbers were determined upon plating of appropriate dilutions of the harvested cultures on agar plates. Total RNA was prepared, separated on a denaturing polyacrylamide gel alongside defined amounts of *in vitro* synthesized SR1 and subsequently, subjected to northern blotting (Figure 7). Losses during RNA preparation were calculated using *in vitro* synthesized SR1 mixed with the same amount of DB104::Δ*sr1* cells at the beginning of the RNA preparation. A comparison with the same amounts of untreated RNA yielded ~80% loss. Loading errors were corrected by reprobing with labelled oligonucleotide C767 complementary to 5S rRNA. Using this quantification procedure, the amount of SR1 within one *B. subtilis* cell was calculated to be ~20 molecules in log phase and 200–250 molecules in stationary phase, corresponding to an approximate intracellular concentration of 30 and 315 nM, respectively.

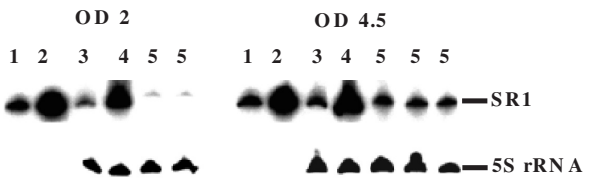

Figure 7. Intracellular concentration of SR1 under different growth conditions. *Bacillus subtilis* strain DB104 was grown to $OD_{560} = 2$ (log phase) or $OD_{560} = 4.5$ (stationary phase), respectively, 5 ml or 1.5 ml culture, respectively, were withdrawn and used for the preparation of total RNA and subsequent northern blotting. Lanes 1 and 2, 6.6 and 33.3 fmol of *in vitro* synthesized, purified SR1, lanes 3 and 4, DB104 (Δ*sr1::cat*) with 6.6 and 33.3 fmol of *in vitro* synthesized, purified SR1 mixed at the beginning of the RNA preparation, lanes 5, two and three parallels of RNA isolated from DB104. An autoradiogram of the northern blot is shown.

DISCUSSION

For all recently discovered trans-encoded sRNAs the targets of which have been identified, only one or two complementary regions were found. In the majority of cases, these regions covered the 5′ part of the target RNA, mostly including the SD sequence, and the mechanism of action was found to be inhibition or activation of translation initiation. Rather unusually, SR1 and *ahrC* mRNA contain seven regions of complementarity that comprise the 3′ half of SR1 and the central and 3′ portion of *ahrC* mRNA (24). This prompted us to determine the secondary structures of SR1 and the *ahrC*/SR1 complex and to investigate the structural requirements for efficient *ahrC*/SR1 pairing.

Figure 1B shows that SR1 is composed of one large 5′ stem-loop (SL1) structure with a prominent bulge, a central small stem-loop SL2 and the terminator stem-loop SL3 separated by two single-stranded regions. Six out of seven regions of complementarity to *ahrC* RNA (B to G) are located in the 3′ 100 nt of SR1. Secondary structure probing of labelled SR1 in complex with increasing concentrations of unlabelled *ahrC* and *vice versa* (Figure 3A and B) revealed structural alterations in six of the seven complementary regions. In SR1, all positions in region C and G as well as a few positions in B, D, E and F were affected (summarized in Figure 3C). In *ahrC*, alterations in regions C, E, F and G as well as additional alterations between regions D and E were found. Interestingly, structural changes over a stretch of ~50 nt were also observed upstream of region G (Figure 3B left), although the *ahrC* SD sequence (nt 21 to 25) and the start codon remained unaffected indicating that binding of SR1 causes structural changes in the 5′ part of *ahrC*-mRNA, too.

Whereas for *cis*-encoded antisense RNAs from plasmids, phages and transposons, a number of studies have been performed to elucidate binding pathways and to determine structural requirements for the two contacting RNA molecules (17), little is known, so far, about the formation of initial contacts between trans-encoded sRNAs and their targets. Here, we show that a solely 78-nt long SR1 species spanning nt 109 to 186 is sufficient for efficient complex formation with *ahrC* mRNA, i.e. the 5′ portion of SR1 is not needed (Figure 2A). Generally, all SR1 species lacking the 5′ half of SL3 with region G or

comprising a complete SL3 were significantly impaired in pairing with *ahrC* RNA. This might indicate that *in vivo* some factor — most likely a protein or an RNase cutting within the loop of SL3 — opens the terminator stem-loop to promote complex formation. Since *in vivo* only full-length $SR1_{205}$ can be observed (northern blots and 3′ RACE, 23), the involvement of an endoribonuclease is highly unlikely. The possibility that the RNA chaperone Hfq that binds upstream of the terminator stem-loop of SR1 is responsible for opening up this structure, can be eliminated, too (see below). Most probably, another, yet unknown RNA-binding protein is needed to open SL3.

Two lines of evidence show that the initial contact between SR1 and *ahrC* RNA occurs at complementary region G of SR1: complex formation assays of truncated SR1/*ahrC* pairs containing mutations and compensatory mutations in region G (Figure 4) and translational *ahrC-lacZ* reporter gene fusions with the same point mutations (Table 2). Furthermore, complex formation assays with SR1 mutants affected in regions C, D, E/F or a combination thereof and a *lacZ* fusion with regions E′, F′ and G′ revealed a contribution of the other complementary regions to SR1/*ahrC* pairing. In summary, since, (i) in the absence of region G, no efficient complex could form, (ii) in the presence of wild-type regions A to E, a 2-nt exchange within G inhibits pairing and (iii) in the presence of G, significant simultaneous alterations in regions C, E and F did affect complex formation, we can conclude, that region G is responsible for the initial contact between SR1 and *ahrC* RNA, but the other complementary regions add to efficient antisense/target RNA pairing.

Region G′ in unpaired *ahrC* mRNA is double-stranded with a bulged-out G at position 116 (Figure 3B left). Interestingly, only when this G and the neighboured C were replaced by a C and G ($ahrC_{88\_G2}$, see Figure 4), the interaction with SR_{186_G2} was restored indicating that it is crucial for the initial contact. As proposed above, some factor is needed to melt or open up region G in SR1, so that the two regions can interact. Our data suggest that pairing initiates at G, but for subsequent steps and stable complex formation, a contribution of the other complementary regions B to F is needed. This is reminiscent of the binding pathway of the antisense/sense RNA pair CopA/CopT involved in regulation of plasmid R1 replication [reviewed in (35)]. Here, binding starts with the interaction of two single-stranded kissing loops and, afterwards, a second region is needed to overcome the torsional stress and to propagate the helix. By contrast, for the antisense/sense RNA pair RNAIII/RNAII of plasmid pIP501, the simultaneous interaction of two complementary loop pairs was found to be required (36). In other cases, a single-stranded region and a loop form the first complex [e.g. Sok/hok of plasmid R1 or RNA-OUT/RNA-IN of transposon IS10, reviewed in (17)].

For many trans-encoded sRNAs in *E. coli*, the RNA chaperone Hfq has been shown to be required for either stabilization of the sRNA or/and efficient duplex formation with the target RNA (see the Introduction section). Previous experiments have demonstrated that Hfq does not stabilize SR1 (24). This report shows that although *B. subtilis* Hfq binds both SR1 and *ahrC* RNA, it is not able to promote complex formation between SR1 and *ahrC* (Figure 5). This is in agreement with data obtained for the RNAIII/*spa* interaction in *S. aureus*, for which Hfq was found to be dispensable for RNAIII/*spa* complex formation (22,16). The fact that no requirement for Hfq was observed in the RatA/*txpA* system of *B. subtilis* (3), too, suggests that in Gram-positive bacteria Hfq might not be needed for sRNA/target RNA interaction or, alternatively, that another RNA chaperone may fulfil the function of Hfq. One candidate might be HBsu, for which RNA-binding activity was demonstrated (37).

However, our previous observation that the levels of the secondary targets of SR1, *rocABC* and *rocDEF* mRNA, were increased 3- to 6-fold in an *hfq* knockout strain (24) raised the question on the role of this chaperone in the SR1/*ahrC* system. Suprisingly, *ahrC* mRNA proved to be not translated in a *B. subtilis hfq* knockout strain (Table 2). This indicates that Hfq is required for efficient translation of *ahrC*, possibly by opening up some secondary structures that otherwise inhibit binding of the 30S initiation complex. This is supported by the finding of one Hfq-binding site (5′ AAAUA) immediately upstream of the *ahrC* ribosome-binding site (RBS). Interestingly, for *E. coli rpoS* mRNA it has been also shown that Hfq is essential for efficient translation (38). In contrast to *ahrC*, the binding of Hfq to SR1 does not seem to play a role in this context. The fact that Hfq binds upstream of six out of seven SR1 regions complementary to *ahrC* mRNA supports the failure of Hfq to promote complex SR1/*ahrC* formation. However, we cannot exclude that Hfq binding might be important for the interaction of SR1 with other, still unidentified target mRNAs.

Based on a series of translational *ahrC-lacZ* fusions, the dispensability of the *ahrC* SD sequence for pairing with SR1 and *in vitro* translation data with chimeric *ahrC*/*sodB* RNAs, we suggested previously that SR1 might affect *ahrC* translation at a post-initiation stage (24). However, the structural alterations found in the *ahrC* mRNA downstream from the SD sequence in the presence of increasing amounts of SR1 prompted us to re-evaluate our previous data using a toeprinting analysis (Figure 6). Both $SR1_{WT}$ and $SR1_{186}$, but not two heterologous RNAs, were able to inhibit binding of the 30S ribosomal subunit and formation of a ternary complex with 30S and $tRNA_f^{Met}$ on full-length *ahrC* mRNA. These results — together with the structure probing data — demonstrate that binding of SR1 induces structural changes in a ~65-nt long stretch of *ahrC* RNA between SD sequence and complementary region G that eventually inhibit formation of the 30S initiation complex. Since the 30S ribosomal subunit covers 54 nt, i.e. 35 (±2) nt upstream and 19 nt downstream from the start codon (39), the 5′ part of the SR1-induced structural alterations of *ahrC* mRNA coincides exactly with this region. The analysis of the G region mutant $SR1_{186\_G2}$ in the toeprinting assay (Figure 6C) corroborated that this region is involved in the first contact between SR1 and *ahrC* mRNA and supported

the specific basepairing interaction between both RNA molecules. The toeprinting results are not opposed to the previously observed translation inhibition of *ahrC-lacZ* fusions (24), as this inhibition can be explained by SR1-induced structural changes in the 5′ part of *ahrC* RNA, too. Therefore, we can conclude that the mechanism of action employed by SR1 is inhibition of translation initiation. This is the first case of a small regulatory RNA that binds ~90 nt downstream from the ribosome-binding site and interferes with translation initiation. In contrast, in the well-studied *E. coli* systems like RyhB/*sodB* (20) or MicA/*ompA* (14,21), the complementary regions between small RNA and mRNA are located upstream of or overlap the target SD sequence, making an effect on ribosome binding and hence, translation initiation, more plausible. Our results raise the question on the maximal distance between SD sequence and a binding region for a small RNA permitting to affect 30S subunit binding. Furthermore, in many *E. coli* cases the inhibition of translation initiation was accompanied by significantly decreased amounts of the target mRNA(s) [e.g. RyhB/*sodB* (40) or SgrS/*ptsG* (41)] that was attributed to degradation of the unprotected target RNA by RNase E or of the complex by RNase III (42). Surprisingly, *ahrC* levels were found to be independent of the presence or absence of SR1 (24). To date, no RNase E has been found in *B. subtilis*. Although two novel endoribonucleases with homology to RNase E, RNase J1 and J2, were recently discovered (43), it is unclear, whether they fulfil the role of the main endoribonucleases as it does RNase E in Gram-negative bacteria.

In the few sense/antisense RNA systems, where calculations of the amount of both interacting species were performed (44,45), an at least 10-fold excess of the inhibitory small RNA over its target was determined. Here, the amount of SR1 in *B. subtilis* grown in complex medium was found to increase upon entry into stationary phase from 15–20 to 250 molecules per cell. This is much lower than the 4500 molecules measured for OxyS under oxidative stress conditions (30), but still in the range of RNAIII of plasmid pIP501 (~1000 molecules). Since we could not detect *ahrC* mRNA in northern blots under any growth condition, its amount must be significantly lower than 15 molecules/cell ensuring at least a 15-fold excess of SR1.

The analysis of the SR1/*ahrC* mRNA interaction yielded three major issues, which might be important for sRNA/target RNA systems in general: First, whereas the major mechanism of action of trans-encoded sRNAs reported in Gram-negative bacteria is inhibition of translation initiation by direct binding to the RBS or 5′ of it, the *B. subtilis* SR1/*ahrC* pair is first case, where translation initiation is prevented by binding of the sRNA ~90 nt downstream from the RBS. Second, while all sRNA/target RNA pairs studied so far comprise at the most two complementary regions, the SR1/*ahrC* pair is the first case with seven complementary regions between inhibitor and target RNA, and the major contribution of one region as well as the minor, but measurable contribution of five of the other regions has been demonstrated. Third, whereas in *E. coli*, Hfq was required for either sRNA stabilization or promotion of complex formation with the target RNA, at least complex formation in Gram-positive bacteria does not seem to depend on Hfq. The search for and analysis of other SR1 targets will reveal whether this sRNA exerts its function(s) by the same or alternative mechanisms.

SUPPLEMENTARY DATA

Supplementary Data are available at NAR Online.

ACKNOWLEDGEMENTS

The authors thank Eckhard Birch-Hirschfeld, Jena, for synthesis of the oligodeoxyribonucleotides and Poul Valentin-Hansen, Odense, for kindly sending us the *E. coli* strains for overexpression of *B. subtilis* Hfq. This work was supported by grant Br1552/6-2 from the Deutsche Forschungsgemeinschaft to S.B. Funding to pay the Open Access publication charges for this article was provided by Deutsche Forschungsgemeinschaft, Project BR1552/6-2.

Conflict of interest statement. None declared.

REFERENCES

1. Storz,G., Altuvia,S. and Wassarman,K.M. (2005) An abundance of RNA regulators. *Annu. Rev. Biochem.*, **74**, 199–217.
2. Vogel,J. and Papenfort,K. (2006) Small noncoding RNAs and the bacterial outer membrane. *Curr. Opin. Microbiol.*, **9**, 605–611.
3. Silvaggi,J.M., Perkins,J.B. and Losick,R. (2005) Small untranslated RNA antitoxin in *Bacillus subtilis*. *J. Bacteriol.*, **187**, 6641–6650.
4. Lee,M., Zhang,S., Saha,S., Santa Anna,S., Jiang,C. and Perkins,J. (2001) RNA expression analysis using an antisense *Bacillus subtilis* genome array. *J. Bacteriol.*, **183**, 7371–7380.
5. Silvaggi,J.M., Perkins,J.B. and Losick,R. (2006) Genes for small, noncoding RNAs under sporulation control in *Bacillus subtilis*. *J. Bacteriol.*, **188**, 532–541.
6. Morfeldt,E., Taylor,D., von Gabain,A. and Arvidson,S. (1995) Activation of alpha-toxin translation in *Staphylococcus aureus* by the trans-encoded antisense RNA, RNAIII. *EMBO J.*, **14**, 4569–4577.
7. Pichon,C. and Felden,B. (2005) Small RNA genes expressed from *Staphyloccoccus aureus* genomic and pathogenicity islands with specific expression among pathogenic strains. *Proc. Natl Acad. Sci. USA*, **102**, 14249–14254.
8. Christiansen,J.K., Nielsen,J.S., Ebersbach,T., Valentin-Hansen,P., Søgaard-Andersen,L. and Kallipolitis,B.H. (2006) Identification of small Hfq-binding RNAs in *Listeria monocytogenes*. *RNA*, **12**, 1–14.
9. Mandin,P., Repoila,F., Vergassola,M., Geissmann,T. and Cossart,P. (2007) Identification of new nonconding RNAs in *Listeria monocytogenes* and prediction of mRNA targets. *Nucleic Acids Res.*, **35**, 962–974.
10. Barrick,J.E., Sudarsan,N., Weinberg,Z., Ruzzo,W.L. and Breaker,R.R. (2005) 6S RNA is a widespread regulator of eubacterial RNA polymerase that resembles an open promoter. *RNA*, **11**, 774–784.
11. Trotochaud,A.E. and Wassarman,K.M. (2005) A highly conserved 6S RNA structure is required for regulation of transcription. *Nat. Struct. Mol. Biol.*, **12**, 313–319.
12. Valentin-Hansen,P., Eriksen,M. and Udesen,C. (2004) The bacterial Sm-like protein Hfq: a key player in RNA transactions. *Mol. Microbiol.*, **51**, 1525–1533.
13. Zhang,A., Wassarman,K.M., Ortega,J., Steven,A.C. and Storz,G. (2002) The Sm-like Hfq protein increases OxyS RNA interaction with target mRNAs. *Mol. Cell*, **9**, 11–22.

14. Rasmussen,A.A., Eriksen,M., Gilany,K., Udesen,C., Franch,T., Petersen,C. and Valentin-Hansen,P. (2005) Regulation of *ompA* mRNA stability: the role of a small regulatory RNA in growth phase-dependent control. *Mol. Microbiol.*, **58**, 1421–1429.
15. Arluison,V., Hohng,S., Roy,R., Pellegrini,O., Regnier,P. and Ha,T. (2007) Spectroscopic observation of RNA chaperone activities of Hfq in posttranscriptional regulation by a small non-coding RNA. *Nucleic Acids Res.*, **35**, 999–1006.
16. Bohn,C., Rigoulay,C. and Bouloc,P. (2007) No detectable effect of RNA-binding protein Hfq absence in *Staphylococcus aureus*. *BMC Microbiol.*, **7**, 10.
17. Brantl,S. (2007) Regulatory mechanisms employed by cis-encoded antisense RNAs. *Curr. Op. Microbiol.*, **10**, 102–109.
18. Schmidt,M., Zheng,P. and Delihas,N. (1995) Secondary structures of *Escherichia coli* antisense MicF RNA, the 5' end of the target *ompF* mRNA, and the RNA/RNA duplex. *Biochemistry*, **34**, 3621–3631.
19. Møller,T., Franch,T., Udesen,C., Gerdes,K. and Valentin-Hansen,P. (2002) Spot 42 RNA mediates discoordinate expression of the *E. coli* galactose operon. *Genes Dev.*, **16**, 1696–1706.
20. Geissmann,T.A. and Touati,D. (2004) Hfq, a new chaperoning role: binding to messenger RNA determines access for small RNA regulator. *EMBO J.*, **23**, 396–405.
21. Udekwu,K.I., Darfeuille,F., Vogel,J., Reimegard,J., Holmqvist,E. and Wagner,E.G.H. (2005) Hfq-dependent regulation of OmpA synthesis is mediated by an antisense RNA. *Genes Dev.*, **19**, 2355–2366.
22. Huntzinger,E., Boisset,S., Saveanu,C., Benito,Y., Geissmann,T., Namane,A., Lina,G., Etienne,J., Ehresmann,B., Ehresmann,C., Jacquier,A., Vandenesch,F. and Romby,P. (2005) *Staphylococcus aureus* RNAIII and the endoribonuclease III coordinately regulate *spa* gene expression. *EMBO J.*, **24**, 824–835.
23. Licht,A., Preis,S. and Brantl,S. (2005) Implication of CcpN in the regulation of a novel untranslated RNA (SR1) in *B. subtilis*. *Mol. Microbiol.*, **58**, 189–206.
24. Heidrich,N., Chinali,A., Gerth,U. and Brantl,S. (2006) The small untranslated RNA SR1 from the *B. subtilis* genome is involved in the regulation of arginine catabolism. *Mol. Microbiol.*, **62**, 520–536.
25. Kawamura,F. and Doi,R.H. (1984) Construction of a *Bacillus subtilis* double mutant deficient in extracellular alkaline and neutral proteases. *J. Bacteriol.*, **160**, 442–444.
26. Heidrich,N. and Brantl,S. (2003) Antisense-RNA mediated transcriptional attenuation: importance of a U-turn loop structure in the target RNA of plasmid pIP501 for efficient inhibition by the antisense RNA. *J. Mol. Biol.*, **333**, 917–929.
27. Stoß,O., Mogk,A. and Schumann,W. (1997) Integrative vector for constructing single-copy translational fusions between regulatory regions of *Bacillus subtilis* and the *bgaB* reporter gene encoding a heat-stable β galactosidase. *FEMS Microbiol. Lett.*, **150**, 49–54.
28. Hartz,D., McPheeters,D.S., Traut,R. and Gold,L. (1988) Extension inhibition analysis of translation initiation complexes. *Methods Enzymol.*, **164**, 419–425.
29. Spedding,G. (1990) Isolation and analysis of ribosomes from prokaryotes, eukaryotes, and organelles. In Spedding,G. (ed), *Ribosomes and Protein Synthesis: A Practical Approach*, IRL Press, Oxford Universtiy Press, New York, pp. 1–29.
30. Altuvia,S., Weinstein-Fischer,D., Zhang,A., Postow,L. and Storz,G. (1997) A small, stable RNA induced by oxidative stress: role as a pleiotropic regulator and antimutator. *Cell*, **90**, 43–53.
31. Benito,Y., Kolb,F.A., Romby,P., Lina,G., Etienne,J. and Vandenesch,F. (2000) Probing the structure of RNAIII, the *Staphylococcus aureus agr* regulatory RNA, and identification of the RNA domain involved in repression of protein A expression. *RNA*, **6**, 668–679.
32. Lease,A.L. and Belfort,M. (2000) A trans-acting RNA as a control switch in *Escherichia coli*: DsrA modulates function by forming alternative structures. *Proc. Natl Acad. Sci. USA*, **97**, 9919–9924.
33. Brantl,S. and Wagner,E.G.H. (1994) Antisense RNA-mediated transcriptional attenuation occurs faster than stable antisense/target RNA pairing: an *in vitro* study of plasmid pIP501. *EMBO J.*, **13**, 3599–3607.
34. Brantl,S. and Wagner,E.G.H. (2000) Antisense-RNA mediated transcriptional attenuation: an *in vitro* study of plasmid pT181. *Mol. Microbiol.*, **35**, 1469–1482.
35. Wagner,E.G.H., Altuvia,S. and Romby,P. (2002) Antisense RNAs in bacteria and their genetic elements. *Adv. Genet.*, **46**, 361–398.
36. Heidrich,N. and Brantl,S. (2007) Antisense RNA-mediated transcriptional attenuation in plasmid pIP501: the simultaneous interaction between two complementary loop pairs is required for efficient inhibition by the antisense RNA. *Microbiology*, **153**, 420–427.
37. Nakamura,K., Yahagi,S., Yamazaki,T. and Yamane,K. (1999) *Bacillus subtilis* histone-like protein, Hbsu, is an integral component of a SRP-like particle that can bind the Alu domain of small cytoplasmic RNA. *J. Biol. Chem.*, **274**, 13569–13576.
38. Muffler,A., Fischer,D. and Hengge-Aronis,R. (1996) The RNA-binding protein HF-I, known as a host factor for phage Qβ RNA replication, is essential for *rpoS* translation in *Escherichia coli*. *Genes Dev.*, **10**, 1143–1151.
39. Hüttenhofer,A. and Noller,H.F. (1994) Footprinting mRNA-ribosome complexes with chemical probes. *EMBO J.*, **13**, 3892–3901.
40. Massé,E., Escorcia,F.E. and Gottesman,S. (2003) Coupled degradation of a small regulatory RNA and its mRNA targets in *Escherichia coli*. *Genes Dev.*, **17**, 2374–2383.
41. Vanderpool,C.K. and Gottesman,S. (2004) Involvement of a novel transcriptional activator and small RNA in posttranscriptional regulation of the glucose phosphoenolpyruvate phosphotransferase system. *Mol. Microbiol.*, **54**, 1076–1099.
42. Afonyushkin,T., Vecerek,B., Moll,I., Bläsi,U. and Kaberdin,V.R. (2005) Both RNase E and RNAse III control the stability of *sodB* mRNA upon translational inhibition by the small regulatory RNA RyhB. *Nucleic Acids Res.*, **33**, 1678–1689.
43. Even,S., Pellegrini,O., Zig,L., Labas,V., Vinh,J., Brechemmier-Baey,D. and Putzer,H. (2005) Ribonucleases J1 and J2: two novel endoribonucleases in *B. subtilis* with functional homology to *E. coli* RNase E. *Nucleic Acids Res.*, **33**, 2141–2152.
44. Brantl,S. and Wagner,E.G.H. (1996) An unusually long-lived antisense RNA in plasmid copy number control: *in vivo* RNAs encoded by the streptococcal plasmid pIP501. *J. Mol. Biol.*, **255**, 275–288.
45. Brenner,M. and Tomizawa,J.-I. (1991) Quantitation of ColE1-encoded replication elements. *Proc. Natl Acad. Sci. USA*, **88**, 405–409.